Quantum path contribution to high-order harmonic spectra

E. Brunetti, R. Issac, and D. A. Jaroszynski
Department of Physics, University of Strathclyde, 107 Rottenrow, G4 0NG Glasgow, United Kingdom
(Received 20 September 2007; published 29 February 2008)

Ultrashort pulses of uv and soft x-ray radiation with durations ranging from femtoseconds to attoseconds can be produced as high-order harmonics of the fundamental frequency of a laser beam focused into gas. Applications to fields such as spectroscopy and attosecond metrology require the control and characterization of spectral and spatial properties of the emitted radiation. These are determined by both single atom and macroscopic response of the interaction medium to the laser field. Here we present evidence that microscopic effects have a larger influence than previously thought, and can induce a splitting and a frequency shift of the harmonic lines. These results not only offer a direct diagnostic for high-order harmonic generation, but also enable us to better tune the parameters of the produced radiation, while giving a deeper insight into the fundamental physics underlying this nonlinear optical process.

DOI: 10.1103/PhysRevA.77.023422 PACS number(s): 32.80.Rm, 42.65.Ky

When atoms are exposed to intense laser radiation, in excess of 10^{13} W/cm^2, electrons are removed from the nucleus, accelerated to very high speeds, and then driven back to the parent ion. In the subsequent high-energy collision, odd harmonics of the laser central frequency are emitted [1,2]. High harmonics are valuable sources of coherent uv and soft x-ray radiation which extend into the water window [3–5], and are offering new tools for time-resolved studies in fields such as biological spectroscopy and lithography [6]. Indeed, a revolution in scientific methodology has been initiated by the availability of attosecond pulses formed from high-order harmonics [7–10], with recent reports of direct time-resolved studies of electronic dynamics [11–14]. Many applications rely on the control of the phase of the harmonics, which depends on the selection of specific electron trajectories. In the present work we have investigated the spectral and spatial properties of harmonics with simulations and experiments, and we show that a signature of the microscopic mechanism responsible for the generation of harmonics can be directly measured as a fine structure in the spectra. Directly probing the electron trajectories allows better control of the characteristics and quality of the generated radiation, enabling fine tuning of its frequency and phase, and opening new opportunities for applications in areas such as spectroscopy and free-electron lasers.

Many aspects of high-order harmonic generation can be explained with a simple three-step model [15], where the laser-atom interaction is separated into ionization, acceleration, and recombination. The laser electric field modifies the binding Coulomb potential allowing the release of an electron into the continuum via tunnel ionization. Successively, it is accelerated by the laser electric field and, depending on the time of ionization, it returns to the proximity of the atomic core where it may recombine and convert the energy gained during its excursion into photons. This model recovers many of the properties of high-order harmonic generation that cannot be explained using perturbative methods, in particular the characteristic spectral shape of the emitted radiation. The spectra typically consist of a plateau of harmonic peaks with approximately constant intensity, followed by a cutoff region, where emission ceases abruptly. This cutoff reflects the maximum energy that the electrons can gain during their trajectory, and above which they do not return to the nucleus.

In the plateau region, several electron trajectories lead to the emission of radiation at the same frequency, but with different temporal and spectral properties. Electrons accelerated just after the peak of a laser cycle return to the nucleus after approximately one period, whereas electrons accelerated later in the pulse follow a trajectory shorter than half a period. Longer trajectories also exist, corresponding to electrons missing the nucleus on the first reencounter, but their contribution to harmonics is weaker. So far, the signature of different trajectories has only been observed indirectly through their influence on the phase of harmonics, which is approximately proportional to the laser intensity, varying with a larger rate for longer trajectories [16]. The shortest trajectory is associated with a slower phase variation and is selected by phase matching when the interaction medium is after the laser focus, where harmonic and laser phase partly compensate [17]. Conversely, longer trajectories are associated with a more rapid phase variation and are more effectively phase matched when the medium is before the focus, and also as off-axis. In this case, harmonics have been found to spectrally broaden and exhibit a lower temporal coherence [18,19]. In addition, the divergence of the emitted radiation, which is determined by the transverse variation of the laser profile, is larger for longer trajectories. This has been observed as regions with different coherence times in interference patterns from high-order harmonic radiation [20]. In this work, we show that contributions from different electron trajectories can be directly identified in harmonic spectra as a splitting of the lines into several components.

Experiments have been performed at the TOPS facility [21] using a 10 Hz, 60 fs, 800 nm Ti:sapphire laser system. The radiation is focused with a 50 cm focal length lens into an Ar gas jet, giving an interaction length of about 1 mm. Harmonics are detected using a soft x-ray spectrometer [22,23] consisting of a gold overcoated concave aperiodic grating which resolves radiation between 5 and 105 nm, and a charge-coupled device (CCD) camera as detector. The grating focuses the radiation in one direction, thus allowing the angular profile of the harmonics to be observed. A 0.8 μm thick Al filter, which transmits about 15% in the range 25–60 nm, prevents saturation of the camera.

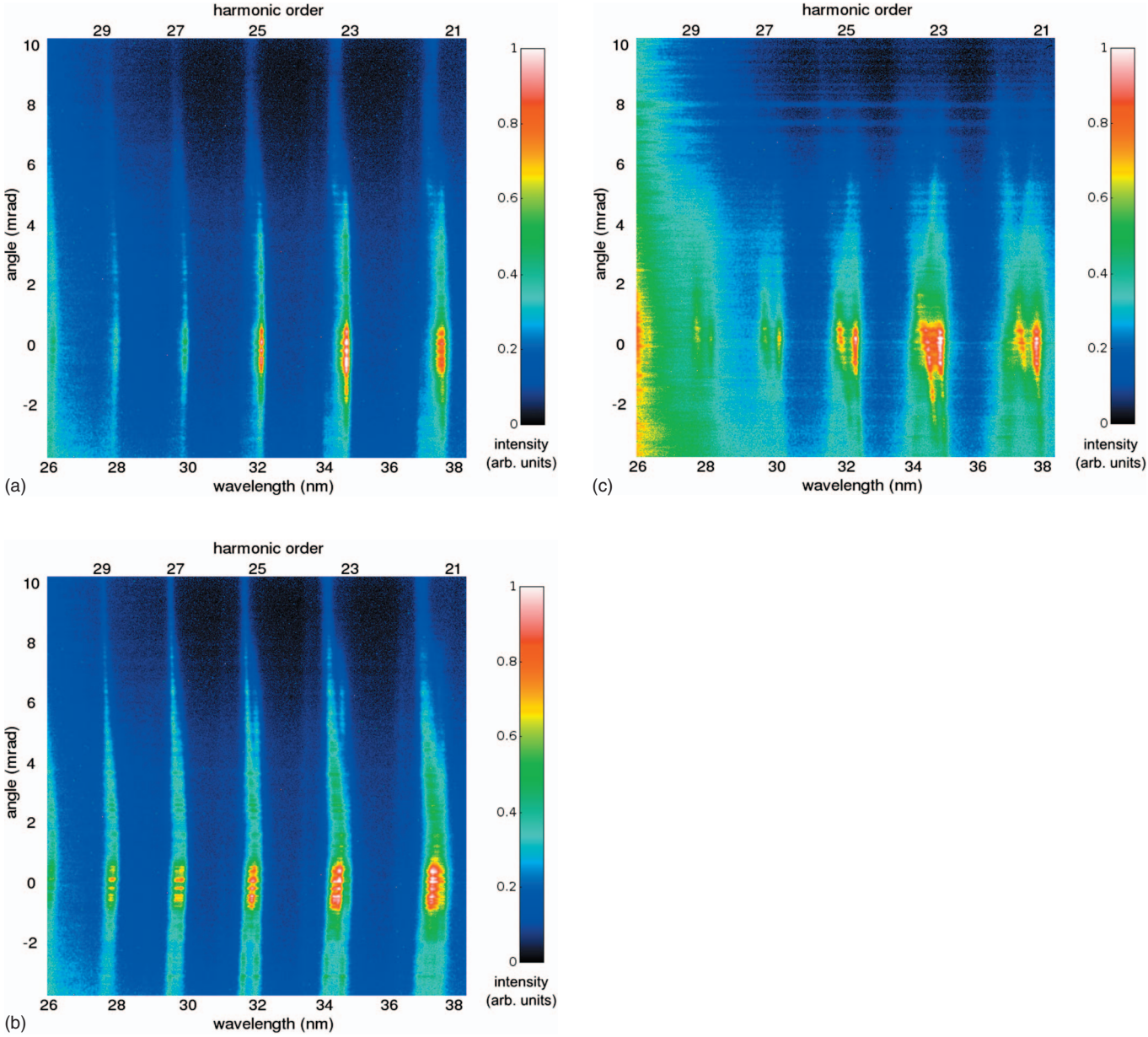

FIG. 1. (Color) Spectra produced with a laser energy of 5 mJ, corresponding to an intensity at the focus of about 1.5×10^{15} W/cm^2. Harmonics with orders between the 21st and the 31st are shown, with the gas jet (a) about 3 mm after the laser focus jet, (b) at the laser focus, and (c) 5 mm before the laser focus. All plots show normalized spectra.

Spectra in Figs. 1 and 2 show the measured far-field profile of harmonics between the 21st and 31st order for three different lens positions: (a) gas jet after the laser focus; (b) at the focus; (c) before the focus. The shape of the harmonic peaks in the three cases are remarkably different, especially for the lower orders, where the lines are considerably broader and split into a number of components. Weak lines are also visible in between the main harmonic peaks.

On axis, the bandwidth $\Delta\omega$ of the harmonics has a typical width of 0.5 rad/fs when the gas jet is after the focus and is broadened to about 1 rad/fs when the focus is moved to behind the gas jet. These values are larger than the laser bandwidth, which is about 0.1 rad/fs, and can be interpreted in terms of the chirp introduced by the temporal variation of the pulse envelope, which is larger when the gas jet is before the focus and longer trajectories are involved. Lines are broader off axis, where phase matching conditions select longer trajectories, which produce radiation over a broader frequency range emitted into a larger cone. It has also been observed that the position of harmonic lines blueshift by about 0.01λ when the gas jet is moved towards the focus, an effect which can be interpreted in terms of ionization induced blueshifting of the laser pulse due to the higher intensity at the focus, where the spot size is smaller.

To help understand our results and to give an insight into the origin of the observed features, we have carried out numerical simulations based on the solution of the one-dimensional Schrödinger equation for an electron in an atom irradiated with intense electromagnetic fields. Our model follows a traditional approach based on the single-active elec-

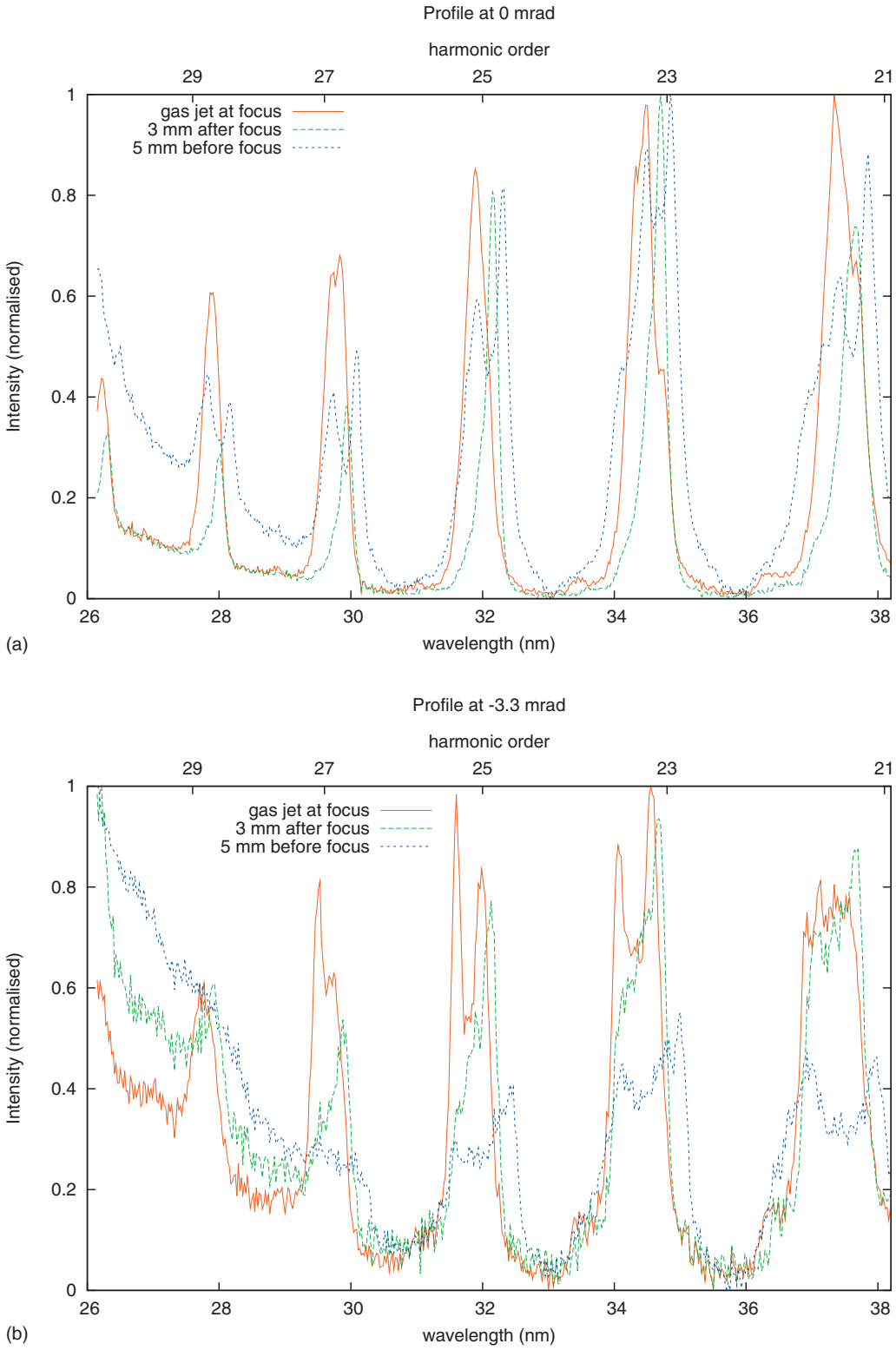

FIG. 2. (Color) Cross sections taken at (a) 0 mrad and (b) −3.3 mrad of the measured spectra shown in Fig. 1. All the curves have been normalized to 1.

tron approximation [2,24] and uses a soft-core potential [25] to model the atomic interaction, in order to remove the singularity of the Coulomb potential in one dimension. The potential has been tuned so that the energy of the ground state matches the first ionization potential of argon. Although one-dimension (1D) models overestimate the ionization rate, the resulting harmonic spectra are in very good agreement with 3D approaches [26], and the short computational times allow the calculation of high resolution spectra for a wide range of parameters. Figure 3 shows a region centered on the 25th

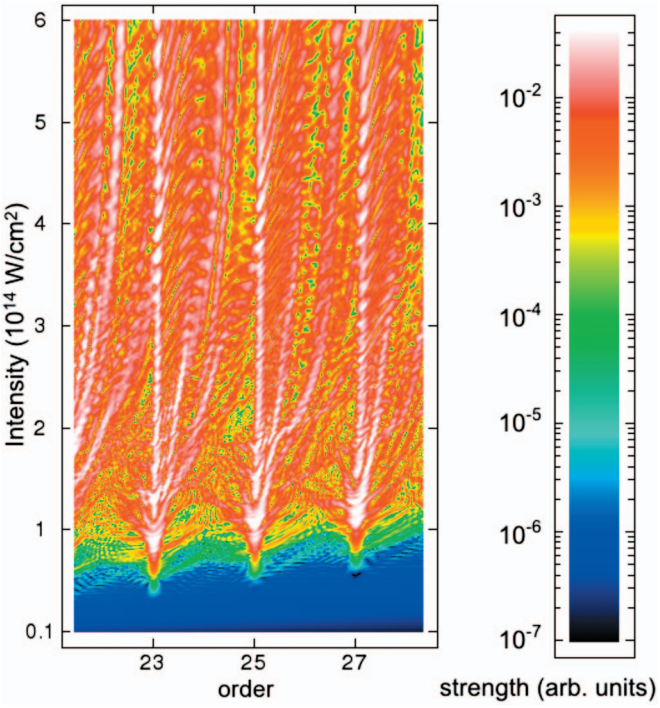

FIG. 3. (Color) Harmonic spectra versus laser intensity for argon interacting with a hyperbolic secant pulse with a duration of 60 fs and a wavelength of 800 nm.

harmonic of spectra produced in the interaction of argon with a 60 fs hyperbolic secant pulse for intensities in the range of (1×10^{13})–(6×10^{14}) W/cm^2. At low intensities, when harmonics are in the cutoff region, peaks are narrow and exhibit no substructure. On the other hand, when the intensity increases and harmonics move into the plateau region, peaks split into several components, some of which are strongly blueshifted. The broadening can be explained by considering that electrons accelerated on the rising edge of the pulse experience an energy boost that translates into a blueshifting of the harmonics, in contrast with a deceleration and a redshifting for electrons accelerated on the falling edge [27]. These redshifted components are also visible, but only for intensities up to about 1.5×10^{14} W/cm^2, beyond which the neutral gas is fully depleted at the peak of the pulse. The amount of shifting is expected to depend on the pulse duration, since the degree of ionization decreases for shorter pulses, and this has been confirmed by our simulations, which show a shift of up to four times the laser frequency for pulses approaching 10 fs. It is worth nothing that this type of blueshifting is purely a single-atom effect, not related to the ionization-induced blueshifting of an intense laser pulse in a plasma [28].

The splitting observed in the plateau region can be better understood by performing a quantum path analysis [29] of the spectra of Fig. 3. This technique relies on the approximately linear relationship, $\phi=\alpha_n I$, between the harmonic phase ϕ and the pump intensity I to extract the contribution α_n of the nth path to harmonics. It has been shown in Ref. [29] that at low intensities, when harmonics are in the cutoff region, only one electron trajectory contributes significantly to the emission of harmonics. In contrast, for increasing laser

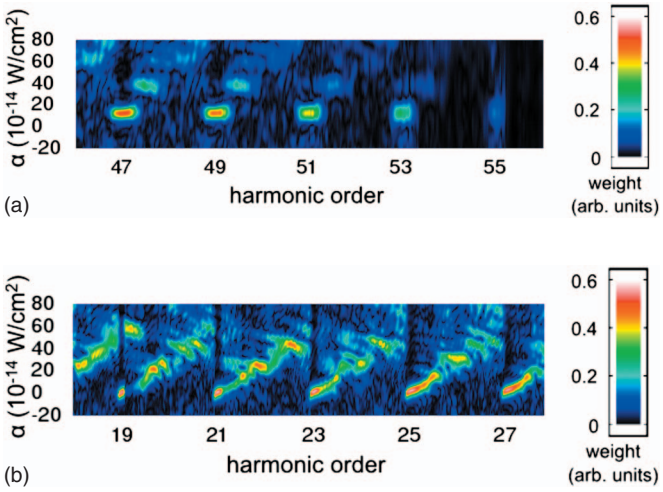

FIG. 4. (Color) Quantum path distribution versus frequency for harmonics generated in argon by a hyperbolic secant pulse with a duration of 60 fs for $I_m=3\times10^{14}$ W/cm^2. (a) Cutoff region, (b) plateau region.

intensities, several trajectories produce radiation at the same wavelength. Here we extend this work by taking "snapshots" at a fixed intensity, and investigating the spectral distribution of radiation generated by electrons following different trajectories. The quantum path distributions for radiation emitted at intensities in the range of about $1-3\times10^{14}$ W/cm^2 are shown in Fig. 4. In the cutoff region, a single spot is visible, corresponding to an electron trajectory with a phase contribution $\alpha\approx12.7$ (in units of 10^{-14} cm^2/W), or $3.2U_p/\omega$, in terms of the pondermotive potential U_p and laser angular frequency ω. In the transition to the plateau, this component splits into two parts at $\alpha\approx1.6$ $(0.4U_p/\omega)$ and $\alpha\approx30$ $(7.6U_p/\omega)$, which are the quantum mechanical counterpart of the two shortest classical trajectories. Contributions from longer trajectories are also visible, corresponding to electrons which miss the nucleus at the first reencounter. Classical calculations predict phase contributions $\alpha\approx25.3$ $(6.4U_p/\omega)$ and $\alpha\approx33.1$ $(8.4U_p/\omega)$ for the second recollision, and $\alpha\approx34.7$ $(8.8U_p/\omega)$ and $\alpha\approx48.4$ $(12.3U_p/\omega)$ for the third recollision, values in good agreement with the results of our simulations.

The splitting observed in Fig. 3 and in the experiments is therefore associated with radiation emitted by electrons following different trajectories, with the core of harmonics predominantly produced by the shortest trajectory and the wings by longer ones. The complex pattern observed in the plateau region is the result of interference occurring when many trajectories produce radiation at the same frequency but with a different phase. This type of quantum interference of space-time electron trajectories is a phenomenon first proposed in calculations of double optical resonance [30] and subsequently observed as multipeak structures in simulated photoelectron spectra for above-threshold ionization (ATI) [31,32], the complementary process to harmonic generation. These effects are difficult to observe in experiments, since they tend to wash out when the contributions from all the atoms forming the medium are summed. However, evidence of quantum interference has been found as fine structure in the angular

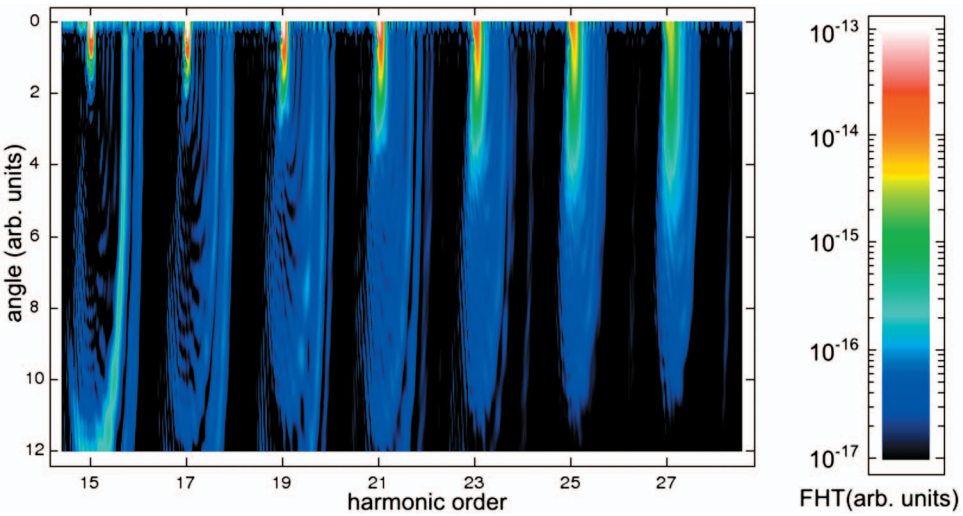

FIG. 5. (Color) Fourier Hankel transform for harmonics generated in argon by a hyperbolic secant pulse with a duration of 60 fs for $I_m = 3 \times 10^{14}$ W/cm^2.

distribution of ATI photoelectrons [33] and in the harmonic spectra shown here.

There are other effects which potentially may distort and broaden the measured spectral lines. One possibility is that the position of the laser focus changes from shot to shot because of pointing instability, thus appearing at the entrance of the spectrometer as apparent wavelength shifts. To eliminate this cause, we have carried out single-shot measurements and observed the same features. Another possible source of broadening is self-phase modulation in the ionizing gas, which could lead to distortion of the laser pulse and the harmonic spectra. However, measurements of the spectrum of the laser after propagating through the gas jet rules this out. As further proof, we have also measured spectra at lower laser energy, when only a small fraction of gas is ionized, and observed the same features, thus eliminating intensity dependent effects. Macroscopically induced splitting has been reported before [34,35], but in experiments performed at higher intensities and with longer pulse durations. For sub-100 fs pulses and for the intensities reached in our measurements, microscopic effects are expected to dominate. A further proof of this is the observed dependence of the splitting on the harmonic order, which does not hold for macroscopically induced splitting. We also performed calculations based on the Fourier Hankel transform of the single-atom data to simulate propagation effects in the low-density weak-focusing regime [36]. An angular-resolved spectra is presented in Fig. 5, showing a very good agreement with our experimental results, including the presence of the weak blueshifted component. In addition to our investigation, the work in [18] found that the harmonic duration increased with broadening of the spectrum, ruling out bandwidth increases due to shortening of the pulse.

In conclusion, we have observed a splitting of the harmonic lines which can be interpreted in terms of radiation emitted by electrons following different microscopic trajectories. The shortest trajectory is associated with a coherent, well-collimated contribution at the core frequencies of harmonic lines, in contrast with broader components predominantly generated by longer trajectories. These have a frequency which can be tuned by adjusting laser and medium parameters, and are better phase matched when the gas jet is before the focus and off axis, due to their fast phase variation. Conversely, the shortest trajectory is better phase matched when the gas jet is after the focus, an ideal condition for applications where higher quality radiation is paramount, e.g., phase locking for the production of attosecond pulses.

We thank David Clark for his technical contribution and acknowledge the support of the UK Research Councils and the Scottish Funding Council.

[1] T. Brabec and F. Krausz, Rev. Mod. Phys. **72**, 545 (2000).
[2] M. Protopapas, C. H. Keitel, and P. L. Knight, Rep. Prog. Phys. **60**, 389 (1997).
[3] E. Seres, J. Seres, F. Krausz, and C. Spielmann, Phys. Rev. Lett. **92**, 163002 (2004).
[4] C. Spielmann, N. H. Burnett, S. Sartania, R. Koppitsch, M. Schnürer, C. Kan, M. Lenzner, P. Wobrauschek, and F. Krausz, Science **278**, 661 (1997).
[5] Z. Chang, A. Rundquist, H. Wang, M. Murnane, and H. Kapteyn, Phys. Rev. Lett. **79**, 2967 (1997).
[6] H. H. Solak, D. He, W. Li, S. Singh-Gasson, F. Cerrina, B. Sohn, M. Yang, and P. Nealey, Appl. Phys. Lett. **75**, 2328 (1999).
[7] I. Osborne and J. Yeston, Science **317**, 765 (2007).
[8] P. B. Corkum and F. Krausz, Nat. Phys. **3**, 381 (2007).
[9] A. Scrinzi, M. Y. Ivanov, R. Kienberger, and D. Villeneuve, J.

Phys. B **39**, R1 (2006).
[10] M. Hentschel, R. Kienberger, C. Spielmann, A. G. Reider, N. Milosevic, T. Brabec, P. Corkum, U. Heinzmann, M. Drescher, and F. Krausz, Nature (London) **414**, 509 (2001).
[11] M. Uiberacker *et al.*, Nature (London) **446**, 627 (2007).
[12] E. Goulielmakis *et al.*, Science **305**, 1267 (2004).
[13] R. Kienberger *et al.*, Nature (London) **427**, 817 (2004).
[14] J. Mauritsson, P. Johnsson, E. Gustafsson, A. L'Huillier, K. J. Schafer, and M. B. Gaarde, Phys. Rev. Lett. **97**, 013001 (2006).
[15] P. B. Corkum, Phys. Rev. Lett. **71**, 1994 (1993).
[16] M. Lewenstein, P. Salières, and A. L'Huillier, Phys. Rev. A **52**, 4747 (1995).
[17] P. Salières, A. L'Huillier, P. Antoine, and M. Lewenstein, Adv. At., Mol., Opt. Phys. **41**, 83 (1999).
[18] P. Salières *et al.*, Science **292**, 902 (2001).
[19] P. Antoine, A. L'Huillier, and M. Lewenstein, Phys. Rev. Lett. **77**, 1234 (1996).
[20] M. Bellini, C. Lyngå, A. Tozzi, M. B. Gaarde, T. W. Hänsch, A. L'Huillier, and C.-G. Wahlström, Phys. Rev. Lett. **81**, 297 (1998).
[21] D. A. Jaroszynski *et al.*, Nucl. Instrum. Methods Phys. Res. A **445**, 317 (2000).
[22] D. Neely, Soft X-ray Spectrometer Operation Manual (2003).
[23] T. Kita and T. Harada, Appl. Opt. **22**, 512 (1983).
[24] J. L. Krause, K. J. Schafer, and K. C. Kulander, Phys. Rev. Lett. **68**, 3535 (1992).
[25] Q. Su and J. H. Eberly, Phys. Rev. A **44**, 5997 (1991).
[26] S. C. Rae, X. Chen, and K. Burnett, Phys. Rev. A **50**, 1946 (1994).
[27] K. J. Schafer and K. C. Kulander, Phys. Rev. Lett. **78**, 638 (1997).
[28] C. Kan, E. Capjack, R. Rankin, and N. H. Burnett, Phys. Rev. A **52**, R4336 (1995).
[29] M. B. Gaarde and K. J. Schafer, Phys. Rev. A **65**, 031406 (2002).
[30] P. Greenland, J. Phys. B **18**, 401 (1985).
[31] J. N. Bardsley, A. Szöke, and M. J. Comella, J. Phys. B **21**, 3899 (1988).
[32] V. C. Reed and K. Burnett, Phys. Rev. A **42**, 3152 (1991).
[33] G. G. Paulus, F. Grasbon, A. Dreischuh, H. Walther, R. Kopold, and W. Becker, Phys. Rev. Lett. **84**, 3791 (2000).
[34] Y. Wang, Y. Liu, X. Yang, and Z. Xu, Phys. Rev. A **62**, 063806 (2000).
[35] Z. Fangchuan, L. Zhong, Z. Zhinan, Z. Zhengquan, L. Ruxin, and X. Zhizhan, Phys. Rev. A **65**, 033808 (2002).
[36] M. B. Gaarde, F. Salin, E. Constant, P. Balcou, K. J. Schafer, K. C. Kulander, and A. L'Huillier, Phys. Rev. A **59**, 1367 (1999).